Revista Internacional de Métodos Numéricos para Cálculo y Diseño en Ingeniería

RIMNI

ARTICLE

Optimal FOPID Controller Design for DC Motor Speed Control Using Ant Lion Optimization Algorithm

Saba Waseem[1], Muhammad Irfan[2,3], Arslan Ahmed Amin[1,*], Saifur Rahman[2,3], Hatim Alwadie[2,3] and Saleh Al Dawsari[2,4,*]

[1]Department of Electrical Engineering, FAST National University of Computer and Emerging Sciences, Chiniot Faisalabad Campus, Punjab, Pakistan
[2]Electrical Engineering Department, College of Engineering, Najran University, Najran, Saudi Arabia
[3]Science and Engineering Research Center, Najran University, Najran, Saudi Arabia
[4]School of Engineering, Cardiff University, Cardiff, UK
*Corresponding Authors: Arslan Ahmed Amin. Email: dr.arslanamin@gmail.com; Saleh Al Dawsari. Email: aldawsarisa@cardiff.ac.uk

Received: 19 October 2025; Accepted: 12 March 2026

ABSTRACT: DC motors are frequently utilized in industrial and automation applications where accurate speed control is crucial. Although conventional Proportional-Integral-and Derivative (PID) controllers are widely utilized, their constant gain values make them less effective in managing dynamic loads and disturbances. It's difficult to get optimal transient and steady-state performance with traditional PID tuning methods. To overcome these limitations, more adaptable and dependable control systems are needed. This study introduces a novel control strategy by optimizing a Fractional-Order PID (FOPID) controller using the Ant Lion Optimization (ALO) method. Mathematical modeling is used to determine the DC motor's transfer function. An ALO, a metaheuristic algorithm, is then implemented to improve five FOPID parameters using Integral Time-weighted Absolute Error (ITAE). The simulation is done in MATLAB-Simulink software. According to the findings, the enhanced ALO-FOPID controller decreased settling time (0.0728 s) and rising time (0.0455 s) when compared to the PID controller, which is taken as a reference. It is noted that the proposed ALO-tuned FOPID demonstrated enhanced response over the conventional methods, demonstrating the usefulness of bio-inspired algorithms for precision control applications. The comparison of the proposed methodology is also done with other studies during different operating conditions. The results show that intelligent optimization-based control in industrial systems is feasible, which aids in the creation of reliable and flexible automation solutions.

KEYWORDS: DC motor speed control; optimization techniques; metaheuristic optimization; ant lion optimization; fractional order PID; transient response

1 Introduction

1.1 Direct Current (DC) Motor Speed Control

DC motors are commonly employed in a range of applications in industries that require a flexible range of angular velocity because of their characteristics, including increased torque, simple control structure, impressive power density, and excellent performance. These uses span electric vehicles, rolling mills, home automation, elevators, robotic manipulators, and aircraft [1]. Unlike induction motors, DC motor controllers operate at cooler temperatures and utilize more affordable driver modules and power components. Researchers have been looking at ways to regulate this

motor's speed since the early 90s, considering how important it is. Fig. 1 shows the DC motor circuit configuration.

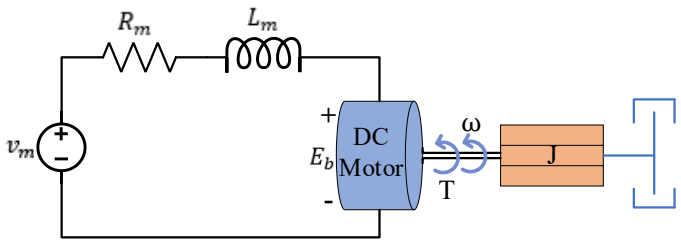

Figure 1: DC Motor circuit configuration [2].

Under constant flux conditions, the $e_b(t)$ (induced voltage) is proportional to the shaft velocity ω(t) multiplied by the back-EMF constant (k_b). Kirchhoff Voltage Law is used to determine $v_m(t)$ (armature voltage) of armature circuit of the DC motor [3]:

$$e_b(t) = k_b \frac{d\theta(t)}{dt} = k_b \omega(t) \quad (1)$$

$$v_m(t) = R_m i_m(t) + L_m \frac{di_m(t)}{dt} + k_b \omega(t) \quad (2)$$

where R_m and L_m denote armature resistance (ohms), and armature inductance (Henry), respectively. T(t) is the DC motor electromagnetic torque, which is proportional to the torque coefficient (k_t), and $i_m(t)$ (armature current), and is found using the formula:

$$T(t) = k_t i_m(t) \quad (3)$$

According to the mechanical dynamic concepts, T(t) can be calculated by summing torques produced by friction and inertia. Thus:

$$T(t) = k_t i_m(t) = J \frac{d\omega(t)}{dt} + B\omega(t) \quad (4)$$

The Laplace transform of the above equations yields the following outcomes, assuming zero initial conditions:

$$E_b(s) = K_b \Omega(s) \quad (5)$$

$$V_m(s) = E_b(s) + I_m(s)(R_m + L_m s) \quad (6)$$

$$T(s) = K_t I_m(s) = (B + Js)\Omega(s) \quad (7)$$

Where B denotes the damping/viscous friction coefficient and J denotes the moment of inertia. Ω(s) (angular speed), and $V_m(s)$ are related by Eqs. (5)–(7). The relationship in Eq. (8) shows the transfer function for the DC motor system. Likewise, input-output relationship between $T_L(s)$ and Ω(s) is represented by $G_{V_m}(s)$ in Eq. (9).

$$G_{TL}(s) = \frac{L_m s + R_m}{K_b K_t + (L_m s + R_m)(Js + B)]}; \text{ when } V_m = 0 \quad (8)$$

$$G_{V_m}(s) = \frac{K_t}{K_b K_t + (L_m s + R_m)(Js + B)]}; \text{ when } T_L = 0 \quad (9)$$

The block diagram of motor model is depicted schematically in Fig. 2, and specifications are provided in Table 1. The parameters are selected similarly to the previous research [3,4].

Table 1: Parameter values of the DC motor.

Parameters	Values
L_m	2.7 H
J	4×10^{-4} kg · m^2
B	0.002 N·m·s/rad
K_t	1.5×10^{-2} N·m/A
R_m	0.4 Ω
K_b	0.05 V·s/rad

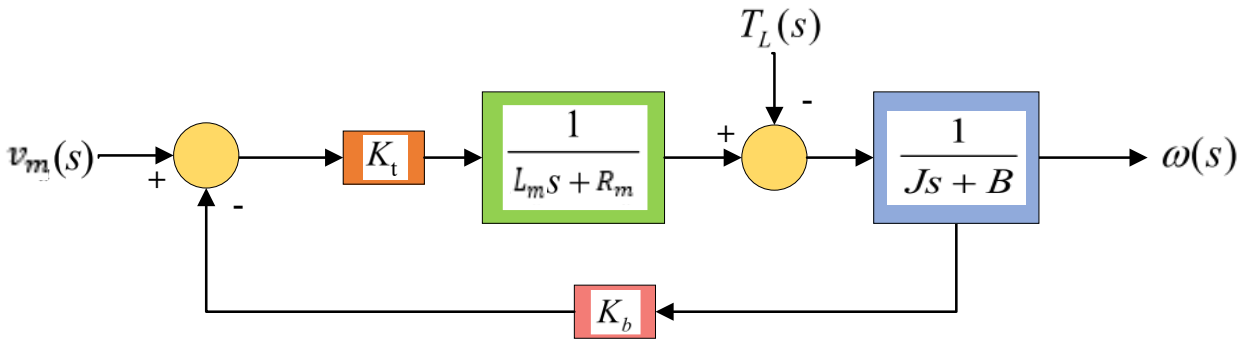

Figure 2: DC Motor Model [2,3].

Maintaining a steady reference for the output of the DC motor, both during normal running conditions and during disturbances, falls under the category of tasks for the control engineer [5]. Changing the power provided to a DC motor will help one to regulate its angular speed [6]. The controller's effectiveness is further hindered by the motors' unexpected and nonlinear properties. So, it's important to check that the final controller can handle variations between the plant and model without compromising performance.

1.2 PID Controller Importance for Speed Control of DC Motor

PID controllers are frequently implemented in industries to improve the response of systems involving a plant or process [7]. Nearly 90% of process industries use PID controllers, according to studies on the topic. The reasons for their popularity include their adaptability, longevity, and ease of use in adjusting control parameters. Although PID controllers have their benefits, they highlight some major drawbacks, such as a delayed reaction caused by changes in load torque, or sensitivity to controller parameters, and an undesirable overshoot in speed as a result of these changes. System model and variable precision are the building blocks of PID controller performance. Balancing the three gains in the correct balance is difficult. Initially, the parameters of the PID controller were tuned either conventionally or via trial-and-error techniques. Not only is it tiresome, but sometimes the best gain levels are difficult to find by trial and error [8,9]. Furthermore, lacking a guarantee of optimal gain values are classical approaches such as ZN and CC, which could lead to undesired oscillation or unexpected overshoot of the system output. External disturbances, load fluctuations, and parametric fluctuations are problems for PI controllers, despite their simple control structure [10,11]. The controller's sensitivity to nonlinearity further complicates fine-tuning the PID gains. Therefore, creating effective control measures to deal with these problems is presently receiving great attention from researchers.

1.3 FOPID Controller Overview

The FOPID controller has two additional terms as compare to typical PID [12]. FOPID controllers require the configuration of these parameters, making the tuning of these controller parameters a challenging task.

Changes to the monitored system and controller parameters have less of an effect on fractional controllers [13]. The iso-damping property, which allows the system response to keep a constant phase margin within a certain frequency range, is easily achieved by a fractional controller. The application of fractional calculus to control theory is extensively discussed in prior literature [14]. One feature of fractional calculus is that it allows the application of real-number orders for integrals and differential operators instead of a fixed integer order. The fundamental operator $\boldsymbol{\alpha}D_t^r$ defines fractional calculus, which involves differentiating and integrating fractional orders. Here, **α** and t refer to the lower and upper limits of the operator, and r denotes the operator's order. The operator described by the continuous integro-differential equation is [15]:

$$\alpha D_t^r = \begin{cases} \frac{d^r}{dt^r} \; for r > 0, \\ 1 \; for r = 0, \\ \int_\alpha^t (dt)^r \; for r < 0, \end{cases}$$

(10)

The fractional integro-differential is represented in literature in a number of ways [16,17]. In the definition of Grunwald-Letnikov, which is given by (11), the binomial coefficient $\binom{\mathrm{r}}{\mathrm{j}}$, a and t are used. The sign of r can be negative or positive, depending on whether referring to an integration context or a differentiation context.

$$\alpha D_t^r f(t) = \lim_{\mathrm{h}\to 0} \mathrm{h}^{-\mathrm{r}} \sum_{j=0}^{\left[\frac{t-a}{h}\right]} (-1)^j \binom{r}{j} \; f\,(t - jh)$$

(11)

The Riemann-Liouville equation is given in its most basic and easily understood form in Eq. (12), where n is an integer and **α** belongs to set of real numbers, and the $\Gamma(.)$ is euler function.

$$\alpha D_t^r f(t) = \frac{1}{\Gamma(n-r)} \frac{d^n}{dt^n} \int \frac{f(\tau)}{(t-\tau)^{r-n+1}} d\tau \qquad (12)$$

Caputo defined integro-differential equations, and this definition is expressed in Eq. (13).

$$\alpha C D_t^r f(t) = \frac{1}{\Gamma(n-r)} \int \frac{f^{(n)}(\tau)}{(t-\tau)^{r-n+1}} d\tau$$

(13)

It's considerably more challenging to express fractional-order differential functions compared to integer-order ones. A function can be made simpler by converting it from a fractional order to an integer order with infinite poles and zeroes. Nonetheless, logical approximation can be used for fractional-order functions that have finite zeros and poles. A simplified approximation method for fractional order functions was proposed by Oustaloup [18] using a recursive distribution of poles and zeros. This fractional order differentiator S^α is defined using the Oustaloup simplified approximation in Eq. (14).

$$S^\alpha = K \prod_{m-1}^{M} \frac{1+s/w_{z,n}}{1+s/w_{z,n}}, \alpha > 0$$

(14)

The gain of the function, K, is adjusted such that it produces a unit gain of 1 rad/sec. From Eqs. (15)–(19), display the recursive equations that are employed to determine the approximate frequency range of zeros and poles. *M* is the symbol for the total number of poles and zeroes. At the nth instant, the system's intended range of lower frequencies (w_l) and higher frequencies (w_h) are represented by the estimated pole and zero frequencies, $w_{z,n}$ and $w_{p,n}$, respectively.

$$w_{z,1} = w_l \sqrt{\eta}$$

(15)

$$w_{p,n} = w_{z,n}\,\gamma \tag{16}$$

$$w_{z,n+1} = w_{p,n}\,\eta \tag{17}$$

$$\gamma = \left(\frac{w_h}{w_l}\right)^{\frac{1-\alpha}{M}} \tag{18}$$

$$\eta = \left(\frac{w_h}{w_l}\right)^{\frac{\alpha}{M}} \tag{19}$$

Eq. (20) represents the generalized FOPID controller transfer function in the s-domain. The equation parameters integral gain constant (K_i), derivative gain constant (K_d), proportional gain constant (K_p), fractional integration order (λ), and fractional derivative order (μ) constitute a total of five variables.

$$G_c(s) = K_p + K_i s^{-\lambda} + K_d s^{\mu} \tag{20}$$

Typically, fractional orders range from zero to two [19]. The generated controller is a standard PID controller for λ equal to 1 and μ equal to 1. A PD controller is produced when λ equals 0, and μ equals 1. A PI controller is characterized by setting λ equal to 1 and μ equal to 0. Eq. (21) defines the FOPID controller equation in the time domain as:

$$u(t) = K_p e(t) + K_i D^{-\lambda} e(t) + K_d D^{\mu}\, e(t) \tag{21}$$

Fig. 3 visually represents the FOPID controller plane in which λ is plotted across the x-axis and μ across the y-axis.

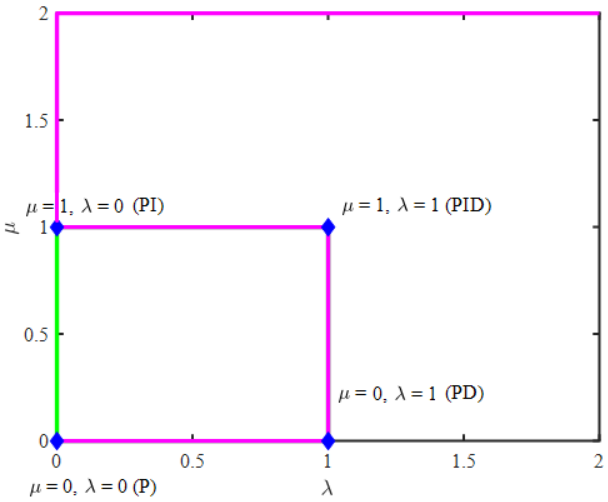

Figure 3: FOPID Plane [20].

This enhancement increases the design flexibility of the controller and facilitates more precise control of real operations [12].

Eq. (22) presents the closed-loop transfer function for a DC motor including unity feedback and an FOPID controller:

$$G_{FOPID}(s) = \frac{K_t(K_i + K_p s^{\lambda} + K_d s^{\mu+\lambda})}{K_t(K_i + K_p s^{\lambda} + K_d s^{\mu+\lambda}) + s^{\lambda}[K_b K_t + (L_m s + R_m)(Js + B)]} \tag{22}$$

Fig. 4 illustrates a system block diagram that controls the speed of a closed-loop DC motor with an FOPID controller. FOPID controllers exhibit reduced steady-state error, decreased percentage overshoot, faster response times, less oscillation, resilience to disturbances, and insensitivity to external changes, in contrast to traditional PID controllers. Applications for FOPID controllers include DC motor control, DC to DC amplifier converters, chaotic system synchronization and control, asynchronous motor drive systems, and magnetic levitation systems.

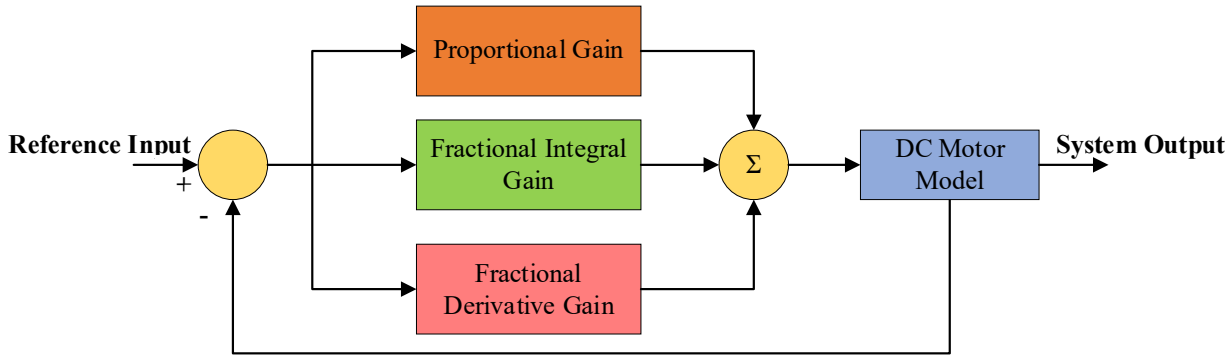

Figure 4: FOPID applied to DC Motor Model [21].

A variety of methods are available for FOPID controllers' tuning [22]. The tuning methods can be grouped as 3 main categories, such as: rule-based procedures, analytical methods, and numerical approaches [19]. The numerical approaches category encompasses parameter tuning strategies that employ heuristic optimization algorithms, frequently utilized by numerous authors in the literature.

1.4 Optimization Techniques for Controller Tuning

Along with the rise in more powerful computers, artificial intelligence (AI)-based optimization techniques have become rather popular. Chen et al. [23] controlled the DC motor speed in an electric car by using a NN-based fuzzy back propagation (BP). By contrast, controlling the FL system and obtaining the appropriate membership functions frequently call for data analysis, model change, and design knowledge [24]. Metaheuristic methods have been implemented in the literature for applications in the past years to ascertain the gains of PID controllers. Metaheuristic algorithms beat conventional approaches in optimizing PID controllers since they can decrease tuning time and improve the likelihood of obtaining optimal gains. Metaheuristic algorithms are methods that replicate chemical, biological, ethnological, or even physical events to address difficult challenges, usually problematic for deterministic methodologies to manage [25]. Although their separate inspiration sources are the most often used, there is no generally agreed-upon criterion for this kind of algorithm [26].

Four groups can be distinguished among metaheuristic algorithms depending on this criterion: algorithms motivated by physics, algorithms based on swarm intelligence, algorithms related to humans, and algorithms inspired by evolution or biology [27]. Some metaheuristic algorithms rely on the mathematical description of physical principles and events. Among the well-known physics-based metaheuristics are Equilibrium Optimizer (EO) [28], Artificial Chemical Reaction Optimization Algorithm (ACROA) [29], Henry Gas Solubility Optimization (HGSO) [30], Gravitational Search Algorithm (GSA) [31], and Heat Transfer Search (HTS) [32]. Swarm intelligence systems replicate the natural big group animal thinking capacity. Among the well-known swarm-intelligence-based metaheuristics are Artificial Bee Colony (ABC) [33], Particle Swarm Optimization (PSO) [34], Ant Colony Optimization (ACO) [35], and Firefly Algorithm (FA) [36]. Mathematical models reflecting different human activities provide the foundation of human-related metaheuristic algorithms. The most considered and often used method in human-based metaheuristics is Teaching-Learning-Based

Optimization (TLBO). Poor and Rich Optimization (PRO) [37], and Doctor and Patient Optimization (DPO) [38] also lie under the human-related metaheuristic algorithms category.

Evolutionary algorithms [39] reflect the concept of biological or natural development. Usually, starting the search process in evolutionary metaheuristics, an initial population is produced at random. Every member of the population's fitness is evaluated utilizing a cost or fitness function. This process continues until the terminating condition is reached [26]. Genetic Algorithm (GA) [40] and Differential Evolution [41] are typically recognized as established metaheuristics within the domain of evolutionary systems.

Various heuristic optimization approaches utilized for the parameter tuning of FOPID controllers related to different applications in literature include GA, PSO, dynamic PSO (dPSO), bacterial swarm optimization (BSO), and simulated annealing (SA). Heuristic optimization techniques primarily offer one advantage over alternative methods: they enable exploration of a broader and more stochastic solution space [42].

1.5 Literature Review

Tuning controller parameters for speed control of a DC motor is a common real-world application of heuristic optimization methods. To adjust the settings of the FOPID controller for DC motor control, GWO [43] and PSO [44] have also been studied in the literature. The conventional PID controller's parameters have been fine-tuned using the following algorithms: GWO [45,46], Intrusive Weed Optimization (IWO) [47], Ant Lion optimization (ALO) [48], Stochastic Fractal Search (SFS) [49], GA [50], Jaya optimization algorithm (JOA) [51], Harris hawks optimization (HHO) [52], and ABC [53]. In comparison to IWO-PID [47], SFS-PID controllers [49], and PSO-PID controllers [44], GWO-based FOPID and GWO-based PID have been developed utilizing the objective function of the integral of time absolute error (ITAE). Decreased settling and rise periods with equivalent overshoot levels were seen when using the GWO-FOPID technique with the ITAE objective function, as compared to alternative approaches. In [44], the PSO-FOPID is built and compared against the PSO-PID using four metrics for performance: Integral Absolute Error (IAE), Integral of Time-weighted Absolute Error (ITAE), Integral Square Error (ISE), and Integral with Time Square Error (ITSE). The results demonstrated that the PSO-FOPID controller outperformed the PSO-PID controller, and that of all the objective functions utilized, the ITAE produced the most favorable outcomes. Using time and frequency response measures, the constrained PSO (CPSO) based FOPID controller with ITSE objective function was developed with 5 distinct output limitations in [54]. Results from MATLAB simulations showed that the CPSO-FOPID achieves better performance than the ZN-based PID controller concerning percentage overshoot, rising time, and settling time. The suggested methods outperformed the more traditional approaches in all of the aforementioned heuristic optimization algorithms for FOPID and PID controllers, including those tuned using ZN, CC, pole location, and phase or gain margin.

According to a study by Musa et al., the ALO in a PID controller could be used to better regulate the velocity of DC motors [48]. The FOPID and PID tuning of DC motor models has also been the subject of some novel approaches. To improve the five FOPID parameters, Hekimoğlu [4] employed the Chaotic Atom Search Optimization (ChASO) algorithm, improving control accuracy and transient response significantly. Eker et al. [55] developed a hybrid approach called Atom Search Optimization-Simulated Annealing (ASO-SA) that combines global search with refinement driven by thermal equilibrium. This allows for efficient tuning of controllers for DC motor systems. The Opposition-Based HGSO (OBL-HGSO) method was proposed by Ekinci et al. [30]. It uses opposition-based learning to enhance delayed convergence. For FOPID optimization in the presence of nonlinear motor dynamics, Ekinci et al. [56] presented the OBL-MRFO-SA hybrid algorithm, which integrates simulated annealing with manta ray foraging dynamics. The Nelder-Mead simplex approach and the Lévy flight distribution are used in a hybrid optimization method proposed by Izci [57] to enhance

the precision of PID controller speed regulation. Lastly, the Gazelle Simplex Optimizer was introduced by Ekinci et al. [58]. This physics-based algorithm takes inspiration from gazelle movement methods and surpasses existing tuning strategies when measuring steady-state performance, response speed, and disturbance rejection. Hence, the literature demonstrates the application of optimization techniques in tuning controller parameters [59].

To maximize FOPID gains and enhance system performance, this research presents a novel approach to DC motor speed control that makes use of the ALO. According to the observations made in the literature, some algorithms like GA, PSO, and ABC can all solve many optimization-related problems, but they have problems with computational burden. If alternative optimization methods were used, better outcomes would be achieved. Furthermore, the result is still going into implementing algorithms for identifying the optimal controller parameter solution in DC motor speed control systems. As a result, research into novel heuristic optimization techniques is needed. Conventional tuning methods, such as ZN or trial-and-error processes, often fail to attain optimal dynamic responsiveness. Also, according to the literature elaborated in previous sections, ALO has received less attention in FOPID tuning research compared to metaheuristic algorithms like PSO and GA. This disparity highlights the need for an improved optimization method to enhance the efficiency of FOPID controllers in controlling the speed of DC motors.

1.6 Ant Lion Optimization (ALO) Algorithm

Designed to address both one-dimensional and multi-dimensional optimization issues, the ALO method is an algorithm that draws inspiration from nature. This algorithm was initially introduced by Mirjalili [60]. Fig. 5 illustrates the working mechanism of the ALO algorithm, emphasizing its iterative process for determining optimal settings.

The larvae of an antlion are concealed beneath the base of a conical hole that the adult digs to capture ants. Because the cone's edge is sharp enough, the ant can easily drop to its base. To keep its prey from escaping the cone, the antlion will force sand outward. After finishing its meal, the antlion would dig a new hole to catch its next meal. The predatory activity of the antlion is divided into five stages: (i) movement of the ant, (ii) building of the trap, (iii) entrapping of the ant in the trap, (iv) capture of prey, and (v) repair of the trap. Because ALO acts like an antlion, which is a predator, certain limitations govern this optimization.

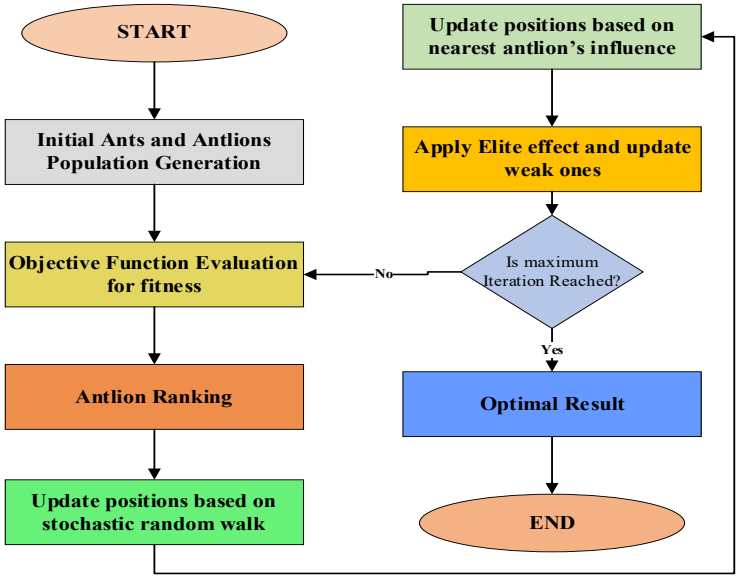

Figure 5: ALO algorithm overview.

1.7 Contribution and Significance of This Research

Changing the controller parameters accurately and reliably is important for regulating the DC motor's speed so that it works at its best under all load conditions. Overshoot, slow response time, and ongoing steady-state inaccuracies are the outcomes of conventional tuning methods' restricted accuracy and adaptability. Although they are effective, current optimization-based tuning methods are either too computationally expensive or don't converge. To overcome these challenges, our proposed work implements the ALO to optimize FOPID controller gains and ensure better speed regulation with minimum error. Without the typical issue of early convergence, which is present in many meta-heuristic algorithms, this method enables effective global search. In comparison to other evolutionary algorithms and conventional optimization methods, ALO achieves more stable convergence while adjusting high-dimensional controller parameters, such as fractional-order gains. ALO also offers a balanced exploration-exploitation approach. FOPID controller optimization presents particular challenges due to nonlinearities, parameter coupling, and performance trade-offs; hence, ALO is a great fit for these problems due to its features. In addition, the comparison findings demonstrate that ALO contributes to enhancing DC motor systems' control accuracy and dynamic performance. This work proposes a novel approach to optimizing FOPID controllers for speed control of a DC motor using the ALO algorithm. Here are the main contributions of this study:

1. An ALO-based optimization framework for FOPID tuning is developed and implemented in MATLAB Simulink. The suggested research improves DC motor speed control systems' accuracy, stability, and flexibility by selecting FOPID parameters optimally using ALO.
2. The enhanced controller's performance in terms of both transient and steady-state characteristics is evaluated, including rise time, overshoot, and settling time. The suggested ALO-FOPID controller is quantitatively assessed in comparison to other existing meta-heuristic optimization techniques from the literature.
3. The performance of the system to maintain the desired input is also illustrated by validating the controller's resilience to load disturbances and different parameter changes.

Our study offers a practical alternative to current tuning methods by improving system dynamics and accelerating convergence. Robotics, industrial automation, and electric vehicle systems that depend on precise motor regulation will all benefit from the findings.

The outline of the next sections is: Section 2 provides the complete research methodology and simulation setup of the suggested approach. The results and related discussion are reported in Section 3. This section also compares ALO-FOPID with alternative tuning approaches in other similar studies. Finally, in Section 4 the research project is concluded, and ideas for future research directions are discussed.

2 Proposed Methodology

2.1 Problem Formulation Modeling

The methodology employed in the proposed work focuses on the control of a DC motor's speed utilizing the ALO algorithm in conjunction with an FOPID controller. Eq. (23) numerically expressed the entire closed-loop system as follows:

$$G_{FOPID}(s) = \frac{K_t(K_i+K_p s^{\lambda}+K_d s^{\mu+\lambda})}{K_t(K_i+K_p s^{\lambda}+K_d s^{\mu+\lambda})+s^{\lambda}[K_b K_t+(L_m s+R_m)(Js+B)]} \quad (23)$$

The numerator signifies the function of the FOPID controller, whilst the denominator denotes the dynamics and influence of the DC motor. The ALO identifies optimal parameter values by

minimizing an objective function, such as the ITAE in this work.

$$\text{ITAE} = \int_0^\infty t|e(t)|dt \tag{24}$$

Below is a list of the detailed stages of the method applied and suggested for the FOPID controller. Input to the system is procedurally generated, five-dimensional ant and lion visuals with a customizable FOPID controller. The output is the ideal value for the FOPID controller settings as found by the systems that perform the best [15].

1. With the controller parameters' boundary values (K_p, K_i, K_d, λ and μ) in mind, initialize the ant population, antlions, and iteration count.
2. The position matrix (M_{ant}) represents the ant colony's location, where *n* is the ant count and *d* is the dimensionality. Here, there is a need to alter five variables in addition to the five control parameters.

$$M_{ant} = \begin{bmatrix} A_{1,1} & \cdots & A_{1,d} \\ \vdots & \ddots & \vdots \\ A_{n.1} & \cdots & A_{n.d} \end{bmatrix} \tag{25}$$

3. The position matrix is considered for evaluating the fitness function of each ant, which is documented in a fitness matrix known as M_{FA}. Here, f is the objective function, *n* represents the variable's number, and *d* is the ant populations.

$$M_{FA} = \begin{bmatrix} f(A_{1,1} & \cdots & A_{1,d}) \\ \vdots & \ddots & \vdots \\ f(A_{n.1} & \cdots & A_{n.d}) \end{bmatrix} \tag{26}$$

4. The antlions' hiding places in the search space are represented by the matrices $M_{antlion}$ and M_{FAL}, which hold the location and fitness value, respectively. Here, *n* represents the total variable's number and antlions.

$$M_{antlion} = \begin{bmatrix} AL_{1,1} & \cdots & AL_{1,d} \\ \vdots & \ddots & \vdots \\ AL_{n.1} & \cdots & AL_{n.d} \end{bmatrix} \tag{27}$$

$$M_{FAL} = \begin{bmatrix} f(AL_{1,1} & \cdots & AL_{1,d}) \\ \vdots & \ddots & \vdots \\ f(AL_{n.1} & \cdots & AL_{n.d}) \end{bmatrix} \tag{28}$$

5. The antlion that corresponds to the best fitness function from M_{FAL} is selected using a roulette wheel.
6. On every cycle, a roulette wheel is used to select an antlion. Eqs. (29) and (30) are used to update the boundary locations proportionally to the current iteration, as shown by the antlion.

$$C^t = \frac{C^t}{I} \tag{29}$$

$$d^t = \frac{d^t}{I} \tag{30}$$

7. In Step 7, a random walk is generated for each ant and uses Eqs. (31) and (32) to normalize their movement within the search space of the decided antlion, and *k* is step index of random walk and *i* is decision variable index.

$$X_k(t) = X_{k-1}(t) + (2r_k(t) - 1), X_0 = 0 \tag{31}$$

$$X_i(t) = \frac{(X_i^t - a_i) \times (d_i^t - C_i^t)}{(b_i - a_i)} + C_i^t \tag{32}$$

8. The ant positions are subsequently adjusted according to Eq. (33).

$$Ant_i^t = \frac{(R_A^t + R_E^t)}{2} \quad (33)$$

9. Next, Eq. (34) is used to determine the fitness values of each ant. If needed, the antlion is switched out for its corresponding ant.

$$Antlion_j^t = Ant_i^t if f(Ant_i^t > f(Antlion_j^t) \quad (34)$$

10. If the antlion's fitness function is better than the ideal, its position is modified.

The steps from 1 through 9 are repeated until the desired number of repetitions has been reached. Each cycle concludes with the best solution. Fig. 6 represents the proposed idea for an ALO-optimized-FOPID control framework in the form of a flowchart implemented for a DC motor speed control application. Constantly interacting with the closed-loop transfer function FOPID, the ALO algorithm proposes several combinations of K_p, K_i, K_d, λ and μ and evaluates their effectiveness based on simulation results.

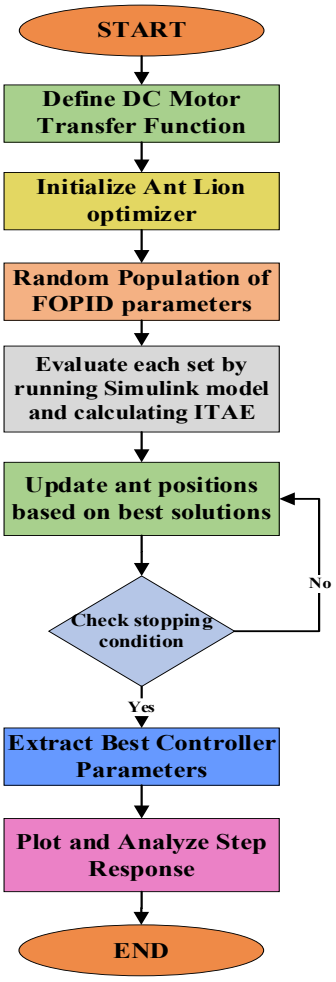

Figure 6: Flowchart of proposed methodology.

The complete proposed control system methodology, using an optimal FOPID controller and the DC motor design, is shown in Fig. 7. A metaheuristic optimization approach is employed to get the optimal values for each of the five gains to optimize the controller. It reduces inaccuracy in the time

domain and improves performance. By lowering the ITAE performance index, which penalizes errors that persist over time, this optimization technique aims to promote faster settling and less steady-state variance. Until the target is met, the optimization process will keep altering the controller gains.

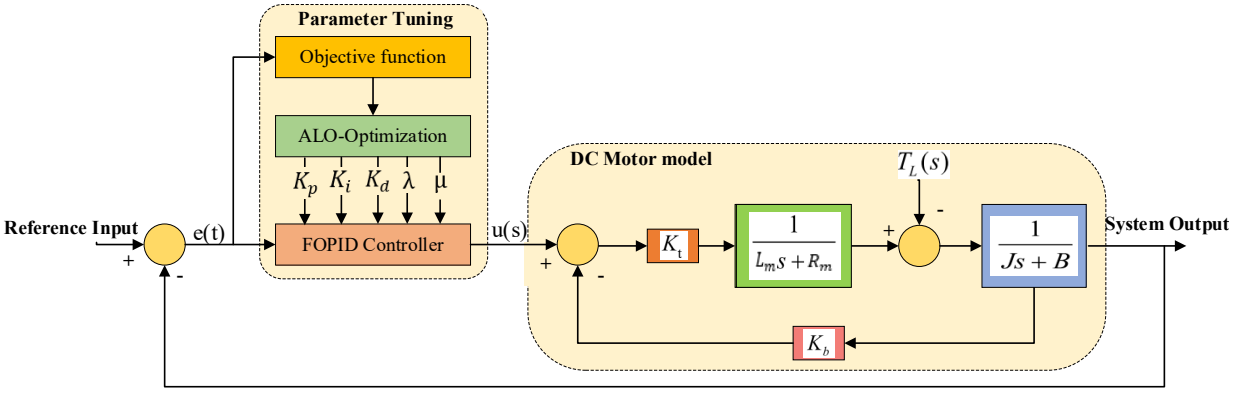

Figure 7: Block diagram of the proposed ALO-FOPID Controller for DC Motor.

2.2 Assumptions of the Work

To ensure compliance with the study's parameters, certain assumptions are considered to facilitate the modeling, analysis, and optimization procedures. Due to their inertia, consistent resistance, damping, and inductance, DC motors are typically regarded as functioning solely in linear conditions. A lumped-parameter linear model is applicable when armature response and magnetic saturation have no impact on the outcomes. Moreover, supposing optimal thermal management overlooks the impact of heat on motor properties, such as temperature-induced resistance. To concentrate exclusively on control performance, we exclude all other variables, including measurement noise, and presume that the load torque remains constant. The sample rates in this system are believed to be sufficiently high to approximate continuous dynamics. The FOPID controller employs fixed rational approximations to produce fractional-order operators, presuming that the specified frequency range encompasses the fundamental dynamics. The ALO method is purported to provide convergence to optimal solutions by judiciously chosen parameters, even in the absence of explicit diversity control strategies [61]. Optimization that disregards computer resource constraints is based on the presumption of enough hardware and convergence duration.

2.3 Limitations of the Work

Despite the technique's overall potential, some limitations may prevent the results from being generalizable [62]. The idealized model ignores nonlinearities that may have an impact on the DC motor's actual performance. These consist of friction, backlash, saturation, and temperature drift. When digital approximations result in phase and gain inconsistencies that are not adequately represented in the simulation model, integrating fractional calculus into real-world systems becomes difficult. Numerous repetitive computations and a narrow range of applications are two of the ALO algorithm's drawbacks. ALO has seen several enhancements in the literature [63]. Even though the ALO approach is still viable, it may converge too quickly in misleading or highly multimodal conditions, producing less-than-ideal tuning outcomes. The optimization does not account for robustness to time-varying disruptions or significant system uncertainties because it is conducted under nominal operating conditions. The proposed FOPID controller is unable to adapt to various operating conditions since its static benefits rely on a limited subset of system characteristics. Ultimately, significant methodological changes will be required to adapt the proposed optimization and control framework to more complex nonlinear or MIMO systems.

3 Results and Discussions

3.1 Simulation of the Reference Model

The purpose of simulating a reference system model of the DC motor with an external PID controller is to provide a performance benchmark. To maintain consistency with earlier published works on control system optimization, this reference model is built using commonly used DC motor characteristics in the literature. Based on previous research, the system parameters, which include armature resistance, inductance, damping coefficient, and rotor inertia, are chosen to mimic a common configuration for small-scale DC motors. With these settings in consideration, the authors simulated the motor's transfer function in MATLAB/Simulink. The closed-loop reference model utilized in the simulation investigation is depicted in Fig. 8 as a block diagram.

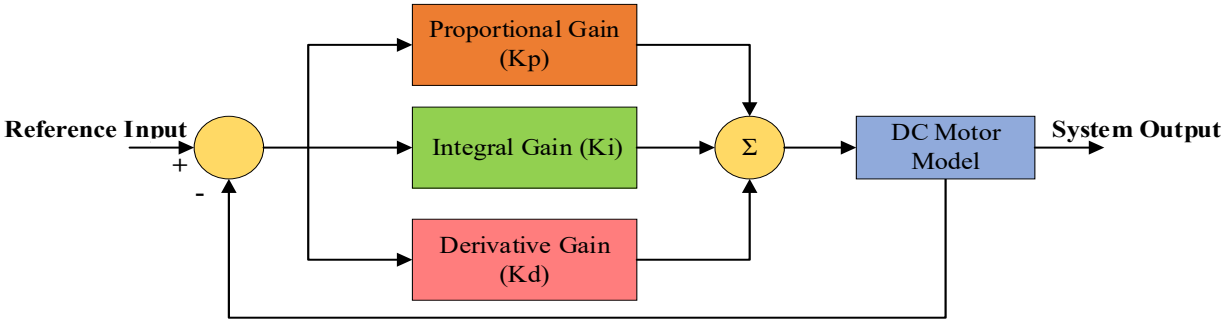

Figure 8: Reference DC motor model with PID controller [64].

Table 2 shows the gain values from the reference model analysis using a PID controller, and Fig. 9 shows the pertinent system response. The MATLAB PID Tuner app was used to fine-tune the PID gains.

Table 2: PID gains.

Parameter	K_p	K_i	K_d
Value	1.909	1.371	0.3791

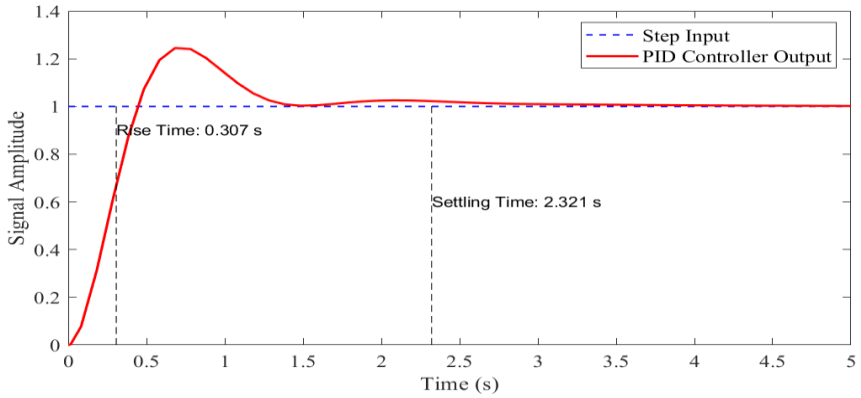

Figure 9: Step response with PID controller.

The system's phase margin (80.8°) and gain margin (18 dB) are assessed using a frequency response analysis. Fig. 10 shows the equivalent Bode plot, which shows the DC motor's inherent stability properties when no optimization is applied. This shows that an improved controller is

required to improve the system's stability and responsiveness because the measured phase margin and gain margin show poor resilience and slow transient performance.

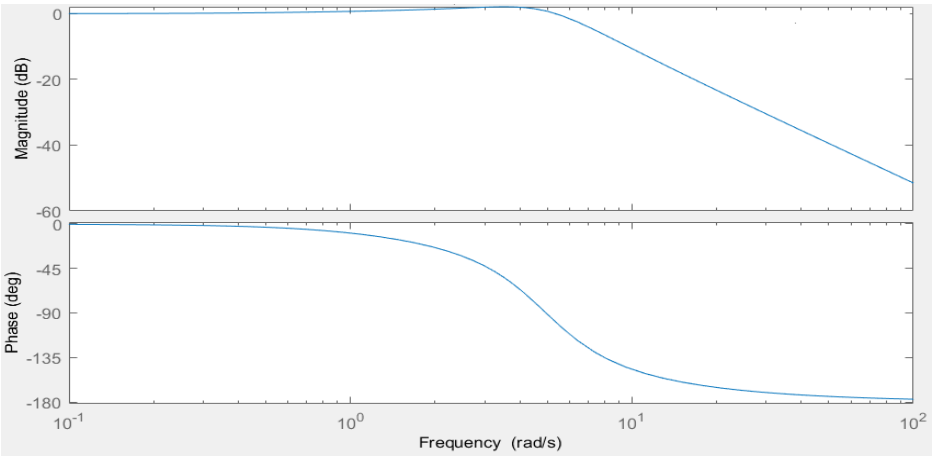

Figure 10: DC motor speed control system Bode plot with PID controller.

Applying a step input to the system allows for additional examination of the reference model in the temporal domain. Important performance measures like rise time, settling time, and % overshoot are derived from the analysis of the output response that follows. A summary of these findings is given in the next subsections. Based on the findings, it is evident that improved control strategies are necessary because the open-loop system displays delayed reaction dynamics and inefficient transient behavior. The efficiency of the suggested FOPID controller, which was modified using the ALO technique, will be evaluated using these baseline values in the results and discussion section.

3.2 Gaps in the Reference Model

The reference model, which is based on the open-loop transfer function of the DC motor, has numerous significant constraints that limit its performance reliability and practical applicability. Despite these shortcomings, it does provide a fundamental understanding of system dynamics. To begin, the model is highly vulnerable to changes in load and outside disturbances due to the lack of feedback management. Lack of dynamic correction mechanisms causes insufficient transient responsiveness, which manifests as long settling periods and significant overrun. Secondly, saturation, dead zones, and friction are nonlinearities that are prevalent in real DC motor systems and are not considered by the reference model. The result is an idealized picture that doesn't always reflect reality. Thirdly, when temperature and load circumstances change, the accuracy of the model could be affected by supposed constant values of its parameters, such as inertia, resistance, damping, etc. Fourth, there are no intelligent or adaptive control mechanisms in the reference model that can respond to changing conditions or account for unexplained dynamics. As a result, the control design is not robust or adaptable. Lastly, the reference model is limited in its efficiency and scalability due to the absence of an optimization mechanism that modifies controller parameters or system performance. These gaps are proposed to be filled with the following contributions in this study:

- Incorporating an optimal FOPID controller with a closed-loop control system.
- ALO is applied for optimal tuning of parameters.
- Accuracy is enhanced in the motor model by incorporating nonlinearities from the real environment.

- To make sure that performance stays the same even in the case of disturbances, response analysis is also implemented.

3.3 Results and Discussion with Proposed Approach

The previously mentioned model of the DC motor was used to simulate the suggested ALO-tuned FOPID controller. It is aimed to enhance the system's performance compared to the open-loop reference model by optimizing the five FOPID parameters. As seen in Fig. 11, the ALO-FOPID controlled system responds far more effectively than the reference model. Table 3 presents the FOPID parameter gains optimized using the ALO algorithm. The ALO technique was employed to determine the settings for the controller, with the ITAE criterion serving as the primary objective. Transient error was successfully reduced using the ALO method's iterative evolution of a population of alternative solutions. Table 4 details the parameters employed by the ALO algorithm in this study. The iterations were limited to 60, and the population size at 70. It was needed to limit the search space for computer performance, and empirical data helped choose these limitations. To maintain convergence, the best answer might be passed down across generations through elite selection. The best cost ITAE obtained after 70 iterations is 0.0018. The optimization result is evaluated using the ITAE. The ITAE value dropped consistently with each iteration using the ALO technique, indicating better FOPID parameters with each cycle. Fig. 12 shows the ITAE convergence curve, which demonstrates this pattern well; it begins with a steep drop in the early iterations. This trend toward convergence proves that the ALO algorithm is stable and efficient at reducing control error and determining the best compromise between rising time, overshoot, and settling performance.

Table 3: FOPID parameter gains.

Parameter	K_p	K_i	K_d	λ	μ
Value	17.298	10.5412	1.5389	0.9508	1.0068

Table 4: ALO algorithm parameters.

Parameter	Value
No. of dimensions	5
No. of agents (Population Size)	70
No. of iterations	60
Lower bounds for K_p, K_i, K_d, λ and μ	[0.001, 0.001, 0.001, 0, 0]
Upper bounds for K_p, K_i, K_d, λ and μ	[20, 20, 20, 2, 2]

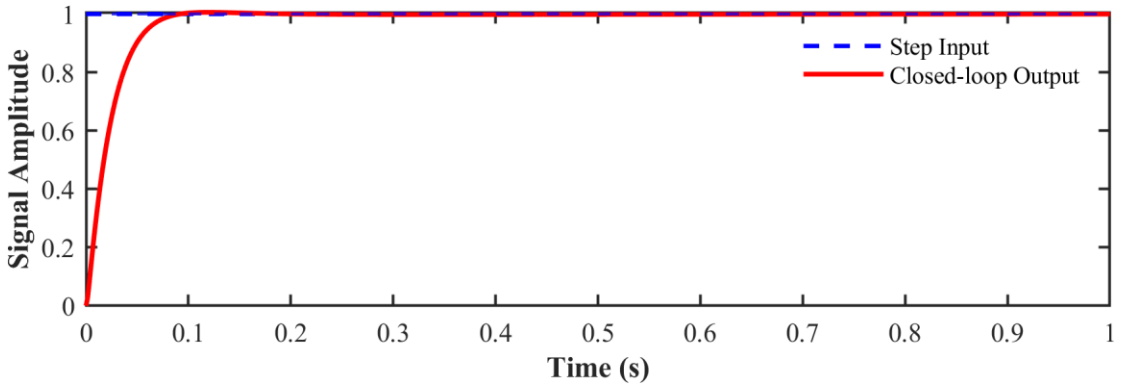

Figure 11: Step response of the DC motor speed with ALO-FOPID.

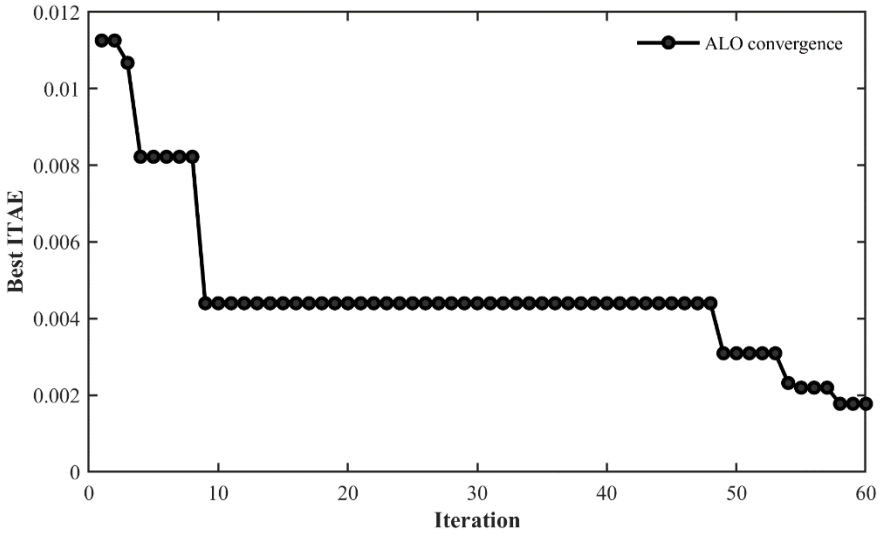

Figure 12: ITAE Convergence Curve.

When compared to its closed-loop equivalent with just a PID controller, the regulated system's step responsiveness is obviously superior. Both the rise and settling times were satisfactory, as seen in Table 5. Table 5's compilation of various metrics makes it easy to see how the model compares to the reference model and this study.

Table 5: Comparison of performance metrics for ALO-FOPID with reference model.

Algorithm-Controller	Rise Time (0.10→0.90)	Settling Time (±2%)	%Overshoot
Reference Model with PID control + without any optimizer	0.307 s	2.321 s	24.2
Proposed Model with FOPID+ALO algorithm	0.0455 s	0.0728 s	0.5787

In addition, the controlled system's Bode plot shows improvement in the stability margin (Fig. 13 and Table 6). With infinite gain margin and 83.1458° phase margin, the closed-loop system appears to be quite stable and durable. In contrast to the ALO's five-parameter tuning guarantee, the FOPID controller's capacity to influence system dynamics throughout a broader frequency range via fractional orders contributes to its longevity. The margins indicate that the ALO-FOPID controller is more stable in the face of disturbances or modifications in the dynamics of the system.

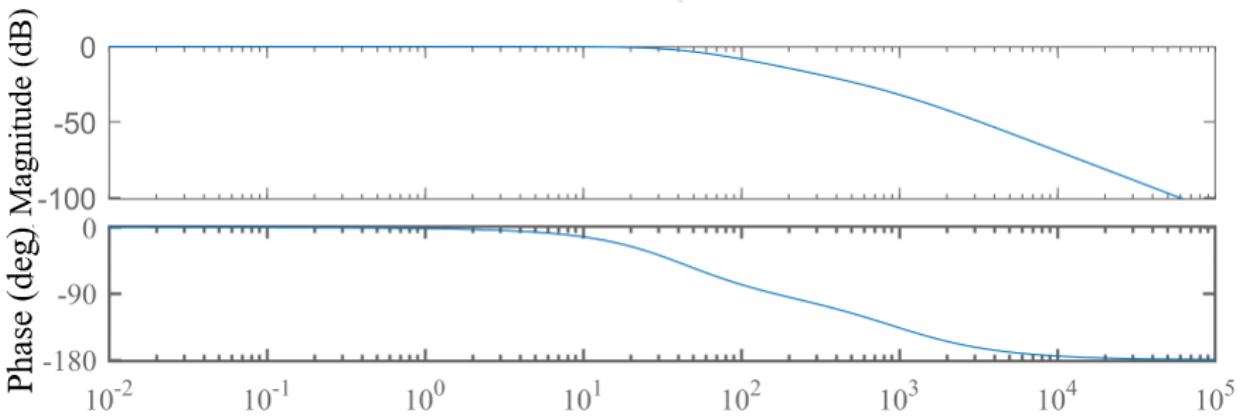

Figure 13: Bode plot with ALO-FOPID controller for DC motor speed control system.

Table 6: Frequency-domain performance comparison.

Algorithm-Controller	Gain margin (dB)	Phase margin (deg.)	Bandwidth (Hz)
ALO-FOPID (proposed)	Infinite	83.1458°	7.4045
ChASO-FOPID [4]	Infinite	179.3515°	84.7989
ASO-FOPID [4]	Infinite	178.3492°	57.0781
GWO-FOPID [43]	Infinite	180°	44.0945
SFS-PID [49]	Infinite	180°	4.1183
OBL-MRFO-SA-FOPID [56]	Infinite	179.5836°	99.4959
MRFO-FOPID [56]	Infinite	179.3445°	60.0777
GSO-PID [58]	Infinite	89.9898°	60.0087

Finally, the suggested ALO-FOPID controller improves the DC motor system's dynamic performance by reducing overshoot, increasing robustness, and obtaining better response. Finding a globally optimal solution in a complex multi-dimensional space demonstrates that the ALO method is suitable for fine-tuning high-dimensional control concerns. These results lend credence to the idea that fractional control and optimization inspired by nature can be useful in precision motor settings.

3.4 Robustness Analysis for a More Significant Evaluation

To strengthen the validity, resilience, and application of the proposed ALO-FOPID control system for DC motor speed regulation, it is crucial to use advanced analytical techniques that expand beyond typical time-domain performance measures. These technological advancements provide more solid proof for decisions, back up theoretical assertions, and shed light on the controller's actions. Among the most important methods is robustness analysis, which evaluates how changes to motor properties, like inductance, resistance, damping, and load torque, impact the system's performance. Showing how robust the controller is against disturbance errors and parameter uncertainty is where this research also contributes.

To evaluate the response of the proposed control system under various motor settings and input conditions, different simulation tests were conducted. Table 7 demonstrates five distinct operating conditions considered. The nominally tuned controller was applied to each scenario without any further adjustments to verify the controller's performance and stability.

Table 7: Time-domain performance comparison.

Condition	Model	Rise Time	Settling Time	% Overshoot
Case No. 1 R_m = 0.30, K_t = 0.012	ALO-FOPID (proposed)	0.0450 s	0.0720 s	0.7400
	ASO-FOPID [4]	0.0474 s	0.0811 s	0.0079
	GWO-FOPID [43]	0.0611 s	0.1022 s	0.2462
	SFS-PID [49]	0.6106 s	0.9247 s	1.8597
	ChASO-FOPID [4]	0.0316 s	0.0536 s	0.0000
	MRFO-FOPID [56]	0.0442 s	0.0725 s	0.0000
	OBL-MRFO-SA-FOPID [56]	0.0442 s	0.0725 s	0.0000
	GSO-PID [58]	0.0453 s	0.0793 s	0.1814
Case No. 2 R_m = 0.30, K_t = 0.018	ALO-FOPID (proposed)	0.0450 s	0.072 s	0.7200
	ASO-FOPID [4]	0.0317 s	0.0516 s	0.0050
	GWO-PID [43]	0.1172 s	0.3469 s	2.3224
	SFS-PID [49]	0.4254 s	0.6412 s	1.5097
	ChASO-FOPID [4]	0.0212 s	0.0335 s	0.1404
	MRFO-FOPID [56]	0.0180 s	0.0467 s	0.4192
	OBL-MRFO-SA-FOPID [56]	0.0180 s	0.0280 s	0.3646
	GSO-PID [58]	0.0304 s	0.0539 s	0.0225
Case No. 3 R_m = 0.40, K_t = 0.015	ALO-FOPID (proposed)	0.0460 s	0.0730 s	0.6500
	ASO-FOPID [4]	0.0379 s	0.0627 s	0.0014
	GWO-FOPID [43]	0.0489 s	0.0816 s	0.3116

	SFS-PID [49]	0.5438 s	1.4458 s	0.0000
	ChASO-FOPID [4]	0.0253 s	0.0408 s	0.0000
	MRFO-FOPID [56]	0.0355 s	0.0564 s	0.1281
	OBL-MRFO-SA-FOPID [56]	0.0214 s	0.0340 s	0.0000
	GSO-PID [58]	0.0365 s	0.0649 s	0.0000
	ALO-FOPID (proposed)	0.0460 s	0.0730 s	0.57000
	ASO-FOPID [4]	0.0472 s	0.0803 s	0.0010
	GWO-FOPID [43]	0.0608 s	0.1013 s	0.2845
Case No. 4	SFS-PID [49]	0.6512 s	1.1073 s	0.0000
R_m = 0.50, K_t = 0.012	ChASO-FOPID [4]	0.0315 s	0.0528 s	0.0000
	MRFO-FOPID [56]	0.0441 s	0.0718 s	0.0000
	OBL-MRFO-SA-FOPID [56]	0.0266 s	0.0437 s	0.0000
	GSO-PID [58]	0.0456 s	0.0808 s	0.0157
	ALO-FOPID (proposed)	0.0460 s	0.0730 s	0.5600
	ASO-FOPID [4]	0.0316 s	0.0514 s	0.0530
	GWO-FOPID [43]	0.0409 s	0.0679 s	0.3702
Case No. 5	SFS-PID [49]	0.4443 s	0.7194 s	0.0000
R_m = 0.50, K_t = 0.018	ChASO-FOPID [4]	0.0212 s	0.0333 s	0.2010
	MRFO-FOPID [56]	0.0029 s	0.0464 s	0.4796
	OBL-MRFO-SA-FOPID [56]	0.0179 s	0.0278 s	0.4264
	GSO-PID [58]	0.0305 s	0.0547 s	0.0000

The performance of the optimized FOPID controller was thoroughly assessed by testing the system under a variety of reference and disturbance settings. The time-domain responses to step, staircase, and sinusoidal reference inputs are displayed in Figs. 14–16, respectively. The suggested controller offers good tracking with less overshoot and settling times, as shown by all test scenarios. As seen in the disturbance rejection experiment in Fig. 17, the controller can maintain a constant output and quickly return to steady-state operation following external disturbances.

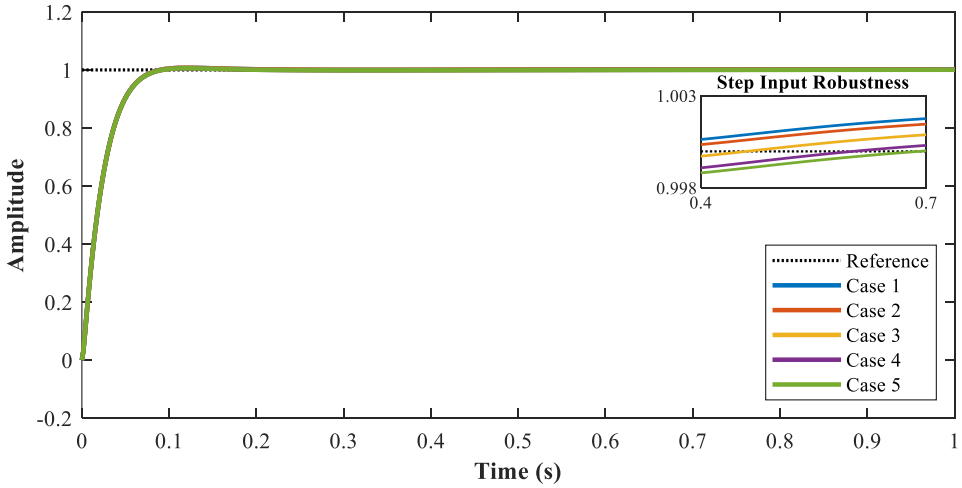

Figure 14: ALO-FOPID-based step input response.

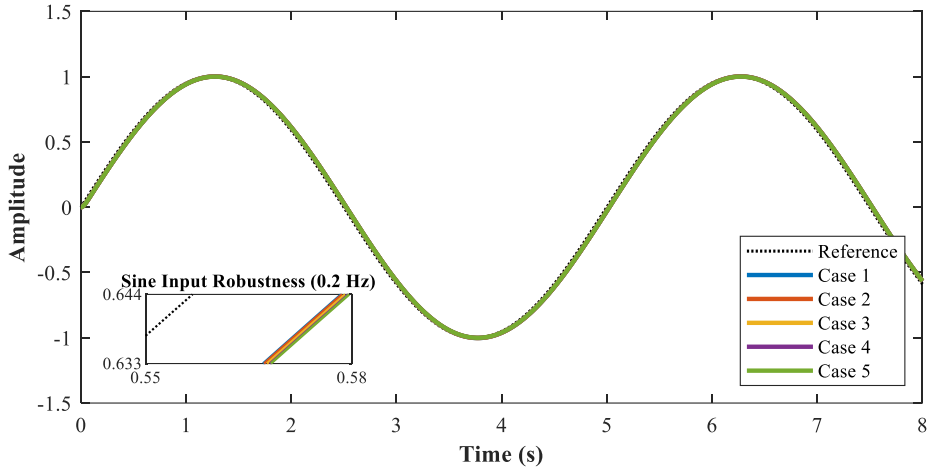

Figure 15: Time domain response of the system for a sine input of 0.2 Hz.

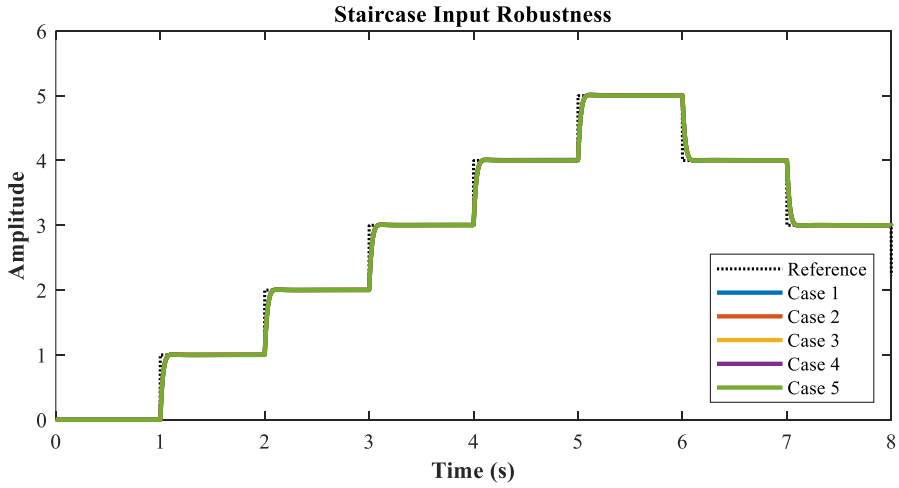

Figure 16: Response of system in case of staircase input.

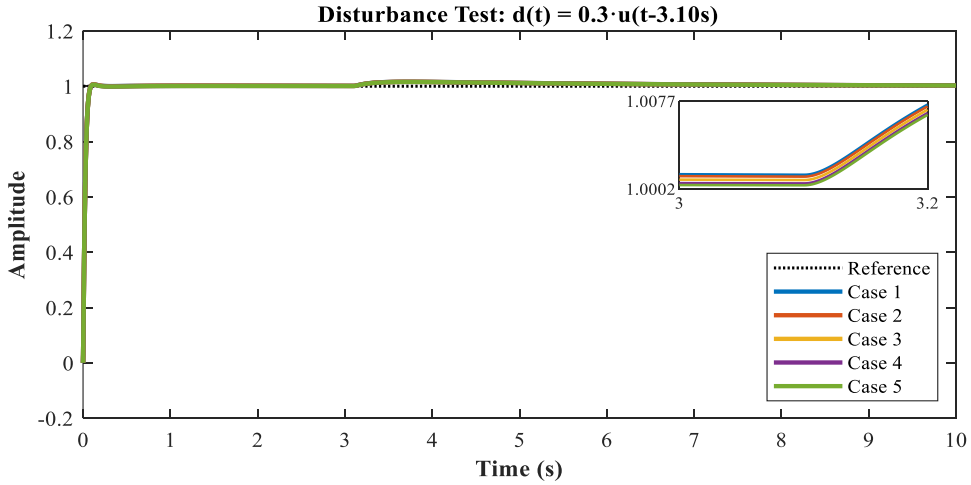

Figure 17: Disturbance input Response.

The adaptability of ALO-tuned FOPID controller is confirmed by consistent performance throughout a range of operating conditions and parameter changes. The responses demonstrate that the proposed ALO-based strategy is appropriate for reliable applications in DC motor speed control because of its suitable tracking accuracy and resilience to uncertainty.

4 Conclusion

This study improved an FOPID controller response for the application of regulating the speed of a DC motor using the ALO technique. A five-parameter FOPID controller was optimized and set to use the ITAE criterion as our objective function. A simulation-based study was conducted to evaluate the controller's performance using MATLAB/Simulink, achieving 0.0455 s rise time and 0.0728s settling time. Notable improvements in time-domain features were seen when comparing the modified ALO-FOPID controller to the original PID controller. In addition, the gain and phase margins became much more stable and robust. It was demonstrated that the ALO algorithm can be used to efficiently tune complex control systems for optimal performance. These results demonstrate the potential of optimization approaches inspired by biology to enhance system dynamics, particularly in industrial automation, and to solve control engineering problems in the real world.

In the future, researchers should explore using hardware platforms like Arduino or dSPACE to implement the ALO-optimized FOPID controller in real-time. To further evaluate robustness, future research should include testing with faults, noise, and disruptions. Possible future applications include expanding the method to nonlinear and MIMO systems and integrating it with smart industrial platforms. Integration of smart industrial control systems with edge computing platforms and the Internet of Things is a promising direction for related future studies.

Acknowledgement: This research was also supported by the National University of Computer and Emerging Sciences- FAST faculty research support through (FRSG-2023) program, Pakistan by providing lab resources.

Funding Statement: The APC of the paper is funded by the School of Engineering, Cardiff University, Cardiff CF24 3AA, UK.

Author Contributions: Conceptualization, Muhammad Irfan, Arslan Ahmed Amin & Saifur Rahman; Formal analysis, Saba Waseem & Arslan Ahmed Amin; Funding acquisition, Arslan Ahmed Amin, Saifur Rahman; Investigation, Saba Waseem, Hatim Alwadie; Methodology, Muhammad Irfan, Arslan Ahmed Amin, Hatim Alwadie & Saleh Al Dawsari; Project administration Muhammad Irfan, Arslan Ahmed Amin, Saifur Rahman Resources, Arslan Ahmed Amin; Software, Arslan Ahmed Amin, Saifur Rahman & Muhammad Irfan, Supervision, Muhammad Irfan, Arslan Ahmed Amin & Saleh Al Dawsari; Validation, Saba Waseem, Hatim Alwadie; Visualization, Arslan Ahmed Amin, Hatim Alwadie & Saleh Al Dawsari; Writing—original draft, Saba Waseem; Writing—review & editing, Muhammad Irfan, Arslan Ahmed Amin, & Saleh Al Dawsari. All authors reviewed and approved the final version of the manuscript.

Availability of Data and Materials: No datasets were generated or analyzed during the current study.

Ethics Approval: Not applicable.

Conflicts of Interest: The authors declare no conflicts of interest.

Abbreviations

ALO	Ant Lion Optimization
DC	Direct Current
FOPID	Fractional-Order Proportional-Integral-Derivative
PID	Proportional-Integral-Derivative
IAE	Integral Absolute Error

ITAE	Integral of Time-weighted Absolute Error
ISE	Integral Square Error
ITSE	Integral with Time Square Error
BSO	bacterial swarm optimization
GA	Genetic Algorithm
DPO	Doctor and Patient Optimization
PRO	Poor and Rich Optimization
TLBO	Teaching-Learning-Based Optimization
FA	Firefly Algorithm
ACO	Ant Colony Optimization
PSO	Particle Swarm Optimization
ABC	Artificial Bee Colony
HTS	Heat Transfer Search
GSA	Gravitational Search Algorithm
HGSO	Henry Gas Solubility Optimization
ACROA	Artificial Chemical Reaction Optimization Algorithm
EO	Equilibrium Optimizer
CC	Cohen-Coon
ZN	Ziegler-Nichols
HHO	Harris Hawks Optimization
JOA	Jaya optimization algorithm
SFS	Stochastic Fractal Search
IWO	Intrusive Weed Optimization
ChASO	Chaotic Ant Search Optimization
SA	Simulated Annealing
MRFO	Manta Ray Foraging Optimization
OBL	Opposition-Based Learning

References

1. University MA, Abut T. Modeling and optimal control of a DC motor. *Int J Eng Trends Technol*. 2016;32(3):146–50. doi:10.14445/22315381/ijett-v32p227.
2. Rajasekhar A, Kunathi P, Abraham A, Pant M. Fractional order speed control of DC motor using levy mutated Artificial Bee Colony Algorithm. In: 2011 World Congress on Information and Communication Technologies. December 11–14, 2011, Mumbai, India. p. 7–13. doi:10.1109/WICT.2011.6141192.
3. Manuel NL, İnanç N, Lüy M. Control and performance analyses of a DC motor using optimized PIDs and fuzzy logic controller. *Results Control Optim*. 2023;13:100306. doi:10.1016/j.rico.2023.100306.
4. Hekimoğlu B. Optimal tuning of fractional order PID controller for DC motor speed control via chaotic atom search optimization algorithm. *IEEE Access*. 2019;7:38100–14. doi:10.1109/ACCESS.2019.2905961.
5. Xu H, Yu D, Wang Z, Cheong KH, Philip Chen CL. Nonsingular predefined time adaptive dynamic surface control for quantized nonlinear systems. *IEEE Trans Syst Man Cybern Syst*. 2024;54(9):5567–79. doi:10.1109/TSMC.2024.3407150.
6. Prathibanandhi K, Ramesh R. Hybrid control technique for minimizing the torque ripple of brushless direct current motor. *Meas Control*. 2018;51(7–8):321–35. doi:10.1177/0020294018786753.
7. Hekimoğlu B, Ekinci S, Kaya S. Optimal PID controller design of DC-DC buck converter using whale optimization algorithm. In: 2018 International Conference on Artificial Intelligence and Data Processing (IDAP). September 28–30, 2018, Malatya, Turkey. p. 1–6. doi:10.1109/IDAP.2018.8620833.
8. Nippatla VR, Mandava S. Performance analysis of permanent magnet synchronous motor based on transfer function model using PID controller tuned by Ziegler-Nichols method. Results Eng. 2025;26:105460. doi:10.1016/j.rineng.2025.105460.
9. Bashishtha TK, Singh VP, Yadav UK, Sahu UK. Fractional-order PID controllers and applications: A comprehensive survey. Annu Rev Control. 2025;60:101013. doi:10.1016/j.arcontrol.2025.101013.
10. Martins OO, Oosthuizen CC, Desai DA. Comparative analysis of evolutionary algorithms for optimising proportional–integral–derivative control in direct current motor speed regulation: A statistical evaluation. J Algorithms Comput Technol. 2025;19:17483026251376985. doi:10.1177/17483026251376985.
11. Maung MM, Latt MM, Nwe CM. DC motor angular position control using PID controller with friction compensation. *Int J Sci Res Publ IJSRP*. 2018;8(11):149–55. doi:10.29322/ijsrp.8.11.2018.p8321.

12. Bourouba B, Ladaci S, Schulte H. Optimal design of fractional order PIλDμ controller for an AVR system using Ant Lion Optimizer. *IFAC-PapersOnLine*. 2019;52(13):200–5. doi:10.1016/j.ifacol.2019.11.304.
13. Podlubny I. Fractional-order systems and PI/sup/spl lambda// D/sup/spl mu//-controllers. *IEEE Trans Autom Control*. 1999;44(1):208–14. doi:10.1109/9.739144.
14. Petráš I. Fractional—Order feedback control of a DC motor. *Journal of Electrical Engineering*. 2099;60: 117–128.
15. Pradhan R, Majhi SK, Pradhan JK, Pati BB. Optimal fractional order PID controller design using Ant Lion Optimizer. *Ain Shams Eng J*. 2020;11(2):281–91. doi:10.1016/j.asej.2019.10.005.
16. Warrier P, Shah P. Fractional order control of power electronic converters in industrial drives and renewable energy systems: A review. *IEEE Access*. 2021;9:58982–9009. doi:10.1109/ACCESS.2021.3073033.
17. Oldham K, Spanier J. The Fractional Calculus—Theory and Applications of Differentiation and Integration to Arbitrary Order. Amsterdam, The Netherlands: Elsevier; 1974 doi:10.1016/s0076-5392(09)x6012-1.
18. A. Oustaloup, La commande CRONE: Commande robuste d'ordre non entier. Paris, France: Hermès; 1991.
19. Shah P, Agashe S. Review of fractional PID controller. *Mechatronics*. 2016;38:29–41. doi:10.1016/j.mechatronics.2016.06.005.
20. Kumar P, Chatterjee S, Shah D, Saha UK, Chatterjee S. On comparison of tuning method of FOPID controller for controlling field controlled DC servo motor. *Cogent Eng*. 2017;4(1):1357875. doi:10.1080/23311916.2017.1357875.
21. Daraz A, Malik SA, Mokhlis H, Haq IU, Zafar F, Mansor NN. Improved-fitness dependent optimizer based FOI-PD controller for automatic generation control of multi-source interconnected power system in deregulated environment. *IEEE Access*. 2020;8:197757–75. doi:10.1109/ACCESS.2020.3033983.
22. Das S, Saha S, Das S, Gupta A. On the selection of tuning methodology of FOPID controllers for the control of higher order processes. *ISA Trans*. 2011;50(3):376–88. doi:10.1016/j.isatra.2011.02.003.
23. Chen W, Lan W, Li X. Research on a control method of DC speed regulating electric energy vehicle based on neural network. In: 2022 3rd International Conference on Computer Vision, Image and Deep Learning & International Conference on Computer Engineering and Applications (CVIDL & ICCEA). May 20–22, 2022, Changchun, China. p. 80–5. doi:10.1109/CVIDLICCEA56201.2022.9824655.
24. Xu H, Dong D, Yu D, Liu YJ. Predefined-time fuzzy adaptive control for spacecraft pose tracking with asymptotic error. *IEEE Trans Fuzzy Syst*. 2025;33(3):971–81. doi:10.1109/TFUZZ.2024.3502360.
25. Ismaeel AAK, Elshaarawy IA, Houssein EH, Ismail FH, Hassanien AE. Enhanced elephant herding optimization for global optimization. *IEEE Access*. 2019;7:34738–52. doi:10.1109/access.2019.2904679.
26. Hashim FA, Houssein EH, Mabrouk MS, Al-Atabany W, Mirjalili S. Henry gas solubility optimization: A novel physics-based algorithm. *Future Gener Comput Syst*. 2019;101:646–67. doi:10.1016/j.future.2019.07.015.
27. Mirjalili S. SCA: A Sine Cosine Algorithm for solving optimization problems. *Knowl Based Syst*. 2016;96:120–33. doi:10.1016/j.knosys.2015.12.022.
28. Faramarzi A, Heidarinejad M, Stephens B, Mirjalili S. Equilibrium optimizer: A novel optimization algorithm. *Knowl Based Syst*. 2020;191:105190. doi:10.1016/j.knosys.2019.105190.
29. Alatas B. ACROA: Artificial Chemical Reaction Optimization Algorithm for global optimization. *Expert Syst Appl*. 2011;38(10):13170–80. doi:10.1016/j.eswa.2011.04.126.
30. Ekinci S, Hekimoğlu B, Izci D. Opposition based Henry gas solubility optimization as a novel algorithm for PID control of DC motor. *Eng Sci Technol Int J*. 2021;24(2):331–42. doi:10.1016/j.jestch.2020.08.011.
31. Rashedi E, Nezamabadi-pour H, Saryazdi S. GSA: A gravitational search algorithm. *Inf Sci*. 2009;179(13):2232–48. doi:10.1016/j.ins.2009.03.004.
32. Patel VK, Savsani VJ. Heat transfer search (HTS): A novel optimization algorithm. *Inf Sci*. 2015;324:217–46. doi:10.1016/j.ins.2015.06.044.
33. Yavuz G, Durmuş B, Aydın D. Artificial bee colony algorithm with distant savants for constrained optimization. *Appl Soft Comput*. 2022;116:108343. doi:10.1016/j.asoc.2021.108343.
34. El-Gammal AAA, El-Samahy AA. A modified design of PID controller for DC motor drives using Particle Swarm Optimization PSO. In: 2009 International Conference on Power Engineering, Energy and Electrical Drives. March 18–20, 2009, Lisbon, Portugal. p. 419–24. doi:10.1109/POWERENG.2009.4915157.
35. Dorigo M, Blum C. Ant colony optimization theory: A survey. *Theor Comput Sci*. 2005;344(2–3):243–78. doi:10.1016/j.tcs.2005.05.020.
36. Li J, Wei X, Li B, Zeng Z. A survey on firefly algorithms. *Neurocomputing*. 2022;500:662–78. doi:10.1016/j.neucom.2022.05.100.
37. Samareh Moosavi SH, Bardsiri VK. Poor and rich optimization algorithm: A new human-based and multi populations algorithm. *Eng Appl Artif Intell*. 2019;86:165–81. doi:10.1016/j.engappai.2019.08.025.

38. Dehghani M, Mardaneh M, Guerrero JM, Malik OP, Ramirez-Mendoza RA, Matas J, et al. A new "doctor and patient" optimization algorithm: An application to energy commitment problem. *Appl Sci*. 2020;10(17):5791. doi:10.3390/app10175791.
39. Mirjalili S, Gandomi AH, Mirjalili SZ, Saremi S, Faris H, Mirjalili SM. Salp Swarm Algorithm: A bio-inspired optimizer for engineering design problems. *Adv Eng Softw*. 2017;114:163–91. doi:10.1016/j.advengsoft.2017.07.002.
40. Ibrahim MA, Mahmood AK, Sultan NS. Optimal PID controller of a brushless DC motor using genetic algorithm. *Int J Power Electron Drive Syst IJPEDS*. 2018;10(2):822. doi:10.11591/ijpeds.v10.i2.pp822-830.
41. Storn R, Price K. Differential evolution–a simple and efficient heuristic for global optimization over continuous spaces. *J Glob Optim*. 1997;11(4):341–59. doi:10.1023/A:1008202821328.
42. Caponetto R, Fortuna L, Fazzino S, Xibilia MG. Chaotic sequences to improve the performance of evolutionary algorithms. *IEEE Trans Evol Comput*. 2003;7(3):289–304. doi:10.1109/TEVC.2003.810069.
43. Agarwal J, Parmar G, Gupta R, Sikander A. Analysis of grey wolf optimizer based fractional order PID controller in speed control of DC motor. *Microsyst Technol*. 2018;24(12):4997–5006. doi:10.1007/s00542-018-3920-4.
44. Jain RV, Aware MV, Junghare AS. Tuning of Fractional Order PID controller using particle swarm optimization technique for DC motor speed control. In: 2016 IEEE 1st International Conference on Power Electronics, Intelligent Control and Energy Systems (ICPEICES). July 4–6, 2016, Delhi, India. p. 1–4. doi:10.1109/ICPEICES.2016.7853070.
45. Madadi A, Motlagh MM. Optimal Control of DC motor using Grey Wolf Optimizer Algorithm [Internet]. 2014 [cited 2026 Jan 1]. Available: https://api.semanticscholar.org/CorpusID:40578138.
46. Bhatnagar U, Gupta A. Application of Grey Wolf Optimization in Optimal Control of DC Motor and Robustness Analysis [Internet]. 2018 [cited 2026 Jan 1]. Available: https://api.semanticscholar.org/CorpusID:160019579.
47. Khalilpour M, Razmjooy N, Hosseini H, Moallem P. Optimal Control of DC motor using Invasive Weed Optimization (IWO) Algorithm. In: Proceedings of the Majlesi Conference on Electrical Engineering; 2011; Isfahan, Iran.
48. Musa MA, T J. Ant lion optimization based PID controller in DC motor speed control. In: 2024 International Conference on Electrical Electronics and Computing Technologies (ICEECT). August 29–31, 2024, Greater Noida, India. p. 1–6. doi:10.1109/ICEECT61758.2024.10738943.
49. Khanam I, Parmar G. Application of SFS algorithm in control of DC motor and comparative analysis. In: 2017 4th IEEE Uttar Pradesh Section International Conference on Electrical, Computer and Electronics (UPCON). October 26–28, 2017, Mathura, India. p. 256–61. doi:10.1109/UPCON.2017.8251057.
50. Taki El-Deen A, Abdel Hakim Mahmoud A, El-Sawi AR. Optimal PID tuning for DC motor speed controller based on genetic algorithm. *Int Rev Autom Control IREACO*. 2015;8(1):80. doi:10.15866/ireaco.v8i1.4839.
51. Achanta RK, Pamula VK. DC motor speed control using PID controller tuned by *Jaya* optimization algorithm. In: 2017 IEEE International Conference on Power, Control, Signals and Instrumentation Engineering (ICPCSI). September 21–22, 2017, Chennai, India. p. 983–7. doi:10.1109/ICPCSI.2017.8391856.
52. Ekinci S, Izci D, Hekimoglu B. PID speed control of DC motor using Harris Hawks optimization algorithm. In: 2020 International Conference on Electrical, Communication, and Computer Engineering (ICECCE). June 12–13, 2020. Istanbul, Turkey. p. 1–6. doi:10.1109/icecce49384.2020.9179308.
53. Mishra AK, Tiwari VK, Kumar R, Verma T. Speed control of DC motor using artificial bee colony optimization technique. In: 2013 International Conference on Control, Automation, Robotics and Embedded Systems (CARE). December 16–18, 2013, Jabalpur, India. p. 1–6. doi:10.1109/CARE.2013.6733772.
54. Roy A, Srivastava S. Design of optimal PIλDδ controller for speed control of DC motor using constrained particle swarm optimization. In: 2016 International Conference on Circuit, Power and Computing Technologies (ICCPCT). March 18–19, 2016, Nagercoil, India. p. 1–6. doi:10.1109/ICCPCT.2016.7530150.
55. Eker E, Kayri M, Ekinci S, Izci D. A new fusion of ASO with SA algorithm and its applications to MLP training and DC motor speed control. *Arab J Sci Eng*. 2021;46(4):3889–911. doi:10.1007/s13369-020-05228-5.
56. Ekinci S, Izci D, Hekimoğlu B. Optimal FOPID speed control of DC motor via opposition-based hybrid *Manta* Ray foraging optimization and simulated annealing algorithm. *Arab J Sci Eng*. 2021;46(2):1395–409. doi:10.1007/s13369-020-05050-z.
57. Izci D. Design and application of an optimally tuned PID controller for DC motor speed regulation via a novel hybrid Lévy flight distribution and Nelder–Mead algorithm. *Trans Inst Meas Control*. 2021;43(14):3195–211. doi:10.1177/01423312211019633.
58. Ekinci S, Izci D, Yilmaz M. Efficient speed control for DC motors using novel gazelle simplex optimizer. *IEEE Access*. 2023;11:105830–42. doi:10.1109/ACCESS.2023.3319596.

59. Kumarasamy V, Karumanchetty Thottam Ramasamy V, Chandrasekaran G, et al. A review of integer order PID and fractional order PID controllers using optimization techniques for speed control of brushless DC motor drive. Int J Syst Assur Eng Manag. 2023;14:1139–1150. doi:10.1007/s13198-023-01952-x.
60. Mirjalili S. The ant lion optimizer. *Adv Eng Softw*. 2015;83:80–98. doi:10.1016/j.advengsoft.2015.01.010.
61. Abualigah L, Shehab M, Alshinwan M, Mirjalili S, Elaziz MA. Ant lion optimizer: A comprehensive survey of its variants and applications. *Arch Comput Meth Eng*. 2021;28(3):1397–416. doi:10.1007/s11831-020-09420-6.
62. Assiri AS, Hussien AG, Amin M. Ant lion optimization: Variants, hybrids, and applications. *IEEE Access*. 2020;8:77746–64. doi:10.1109/ACCESS.2020.2990338.
63. Chen SC, Huang WC, Hsueh MH, Pan CY, Chang CH. A novel exponential-weighted method of the antlion optimization algorithm for improving the convergence rate. *Processes*. 2022;10(7):1413. doi:10.3390/pr10071413.
64. Güven AF, Mengi OÖ, Elseify MA, Kamel S. Comprehensive optimization of PID controller parameters for DC motor speed management using a modified jellyfish search algorithm. *Optim Control Appl Meth*. 2025;46(1):320–42. doi:10.1002/oca.3218.